



VICTORIA UNIVERSITY
MELBOURNE AUSTRALIA

FKBP25 regulates myoblast viability and migration and is differentially expressed in in vivo models of muscle adaptation

This is the Published version of the following publication

Cree, Tabitha, Gomez, Tania Ruz, Timpani, Cara, Rybalka, Emma, Price, John and Goodman, Craig (2023) FKBP25 regulates myoblast viability and migration and is differentially expressed in in vivo models of muscle adaptation. *The FEBS Journal*, 290 (19). pp. 4660-4678. ISSN 1742-464X

The publisher's official version can be found at
<https://febs.onlinelibrary.wiley.com/journal/17424658>
Note that access to this version may require subscription.

Downloaded from VU Research Repository <https://vuir.vu.edu.au/47788/>

FKBP25 regulates myoblast viability and migration and is differentially expressed in *in vivo* models of muscle adaptation

Tabitha Cree^{1,2}, Tania Ruz Gomez¹, Cara A. Timpani^{1,2}, Emma Rybalka^{1,2}, John T. Price^{1,2,3,4} 
 and Craig A. Goodman^{1,2,5} 

1 Institute for Health and Sport (IHeS), Victoria University, Melbourne, Australia

2 Australian Institute for Musculoskeletal Science (AIMSS), St Albans, Australia

3 Department of Biochemistry and Molecular Biology, Monash University, Clayton, Australia

4 Monash Biomedicine Discovery Institute, Clayton, Australia

5 Department of Physiology, Centre for Muscle Research (CMR), The University of Melbourne, Parkville, Australia

Keywords

FKBP25; muscle adaptations; myoblast; proliferation; tubulin dynamics

Correspondence

C. A. Goodman, Centre for Muscle Research, The University of Melbourne, Parkville, Vic. 3010, Australia
 E-mail: craig.goodman@unimelb.edu.au

(Received 1 September 2022, revised 18 April 2023, accepted 21 June 2023)

doi:10.1111/febs.16894

FKBP25 (FKBP3 gene) is a dual-domain PPIase protein that consists of a C-terminal PPIase domain and an N-terminal basic tilted helix bundle (BTHB). The PPIase domain of FKBP25 has been shown to bind to microtubules, which has impacts upon microtubule polymerisation and cell cycle progression. Using quantitative proteomics, it was recently found that FKBP25 was expressed in the top 10% of the mouse skeletal muscle proteome. However, to date there have been few studies investigating the role of FKBP25 in non-transformed systems. As such, this study aimed to investigate potential roles for FKBP25 in myoblast viability, migration and differentiation and in adaptation of mature skeletal muscle. Doxycycline-inducible FKBP25 knockdown in C2C12 myoblasts revealed an increase in cell accumulation/viability and migration *in vitro* that was independent of alterations in tubulin dynamics; however, FKBP25 knockdown had no discernible impact on myoblast differentiation into myotubes. Finally, a series of *in vivo* models of muscle adaptation were assessed, where it was observed that FKBP25 protein expression was increased in hypertrophy and regeneration conditions (chronic mechanical overload and the *mdx* model of Duchenne muscular dystrophy) but decreased in an atrophy model (denervation). Overall, the findings of this study establish FKBP25 as a regulator of myoblast viability and migration, with possible implications for satellite cell proliferation and migration and muscle regeneration, and as a potential regulator of *in vivo* skeletal muscle adaptation.

Introduction

Peptidyl prolyl isomerases (PPIase), which include the FK506 binding proteins (FKBPs), are a class of enzymes that facilitate the conversion of peptide bonds between proline residues from *cis* to *trans*

conformations [1]. The unusual conformation of the cyclic proline side chain leads to steric hindrance of the growing polypeptide chain, such that the non-binding interaction of the *cis*-proline side chain impairs the

Abbreviations

25KD, FKBP25 knockdown; BTHB, Basic tilted helix bundle; Dox, doxycycline; FKBP25, FK506 binding protein 25; *mdx*, murine muscular dystrophy; Mir, MicroRNA; MT, microtubule; MTE, myotectomy; MTORC1, mechanistic target of rapamycin complex 1; MyHC, myosin heavy chain; PPIase, peptidyl prolyl isomerase; SA, synergist ablation.

ability of the peptide chain to bind to additional amino acids and form a secondary structure [2,3]. Proline isomerisation can also occur as a regulatory modification of selected proteins to modulate their function, including histone H3 [4], RNA polymerase II [5] and mitogen-activated protein kinase (MAPK/p38) [6].

FKBPs are a diverse family of immunophilin molecules that range in size and function (for review see [7,8]). The most well known is FKBP12 (FKBP1A gene) which mediates immune suppression when complexed with the immunosuppressant drug, FK506 (Tacrolimus) [9], and plays a role in the inhibition of the mechanistic target of rapamycin complex 1 (mTORC1) signalling when complexed with rapamycin [10]. The function of the FKBPs is dependent on their structure and presence of functional domains, including the PPIase domain, PPIase-like domain and tetrapeptide (TPR) domain, which can be found in large FKBPs [11]. While the function of large FKBPs, including FKBP51 and FKBP52, has been extensively studied [12–17], other FKBPs, such as FKBP25, are yet to be thoroughly investigated.

FKBP25 (FKBP3 gene) is a dual-domain protein consisting of a C-terminal PPIase region and an N-terminal basic tilted helix bundle (BTHB) region [18]. From the relatively few studies that have investigated FKBP25's structure and function, it has been found that the PPIase domain is required for protein binding activity and the BTLB domain is needed to facilitate nucleic acid binding [18]. Consistent with this, FKBP25 has been demonstrated to shuttle between the cytoplasm and the nucleus and be involved in nucleic acid binding, DNA repair and interaction with pre-60S ribosomal subunits [19–22]. Recently, FKBP25 has also been found to bind to microtubules, via its catalytic domain, regulating tubulin polymerisation and mitotic spindle dynamics during the cell cycle [23], suggesting that FKBP25 has the potential to regulate cell proliferation and/or cell migration. Indeed, two recent studies have shown that the knockdown of FKBP25 reduces breast and lung cancer cell proliferation and invasion properties [24,25]; however, studies on the role of FKBP25 in cell proliferation and migration in non-transformed cells are lacking.

Interestingly, a recent quantitative proteomics study found that FKBP25 is the mostly highly expressed of all FKBPs in mature mouse skeletal muscle and is in the top 25% most highly expressed proteins in the muscle proteome [26]. To date, however, no studies have specifically examined the role and regulation of FKBP25 in muscle cells or in mature skeletal muscle. Therefore, this study examined the expression of FKBP25 in proliferating, differentiating and quiescent myoblasts, the role of FKBP25 in myoblast accumulation/viability, migration and differentiation, and changes to the expression of FKBP25 in various *in vivo* models of adaptation in mature skeletal muscle.

Results

FKBP25 protein expression is associated with proliferative potential of C2C12 myoblasts

Myogenesis is the process of proliferative myoblasts fusing together and differentiating into myotubes (*in vitro*) or mature muscle fibres (*in vivo*) [27]. Upon induction of myoblast differentiation, a cascade of myogenic regulatory factors (MRFs) begin to be transcribed to facilitate the transition to mature myotubes, including myoblast determination protein 1 (MyoD) and myogenin [28]. These factors are repressed in proliferative myoblasts and are activated upon induction of differentiation by cessation of cyclin-dependent kinase activity corresponding to the withdrawal of myoblasts from the cell cycle to undergo terminal differentiation. To determine whether FKBP25 abundance would be altered during myogenesis, we examined FKBP25 protein expression in C2C12 myoblasts over a 96-h time course from the initiation of differentiation by serum deprivation (Fig. 1). As shown in Fig. 1A,B, differentiation resulted in the expected progressive formation of multi-nucleated myotubes. Corresponding to the withdrawal from the cell cycle, myotube formation was associated with a decreased expression of Cyclin D1, and increases in MyoD, myogenin and myosin heavy chain proteins. Importantly, differentiation was also associated with significant increase expression in FKBP25 protein

Fig. 1. FKBP25 protein increases during C2C12 myoblast differentiation and is ubiquitously expressed throughout the cytoplasm and nucleus of C2C12 myoblasts. Proliferating C2C12 myoblasts were induced to differentiate in media containing 2% horse serum for up to 96 h. (A) C2C12 morphology throughout differentiation from an immature myoblast cell to mature myotube (i–iv; images taken at 10× magnification. Scale bar = 100 μm). (B) Representative western blots of FKBP25 expression, myogenic and proliferation markers. (C) FKBP25 expression increases throughout C2C12 myogenesis, represented by one-way ANOVA with Tukey's *post hoc* test. (D) FKBP25 is ubiquitously expressed throughout the cytoplasm and nucleus of C2C12 myoblasts (i) and myotubes (ii) (images taken at 60× magnification. Scale bar = 10 μm). Data are presented as mean ± SD of $n = 3$, * = $P \leq 0.05$.

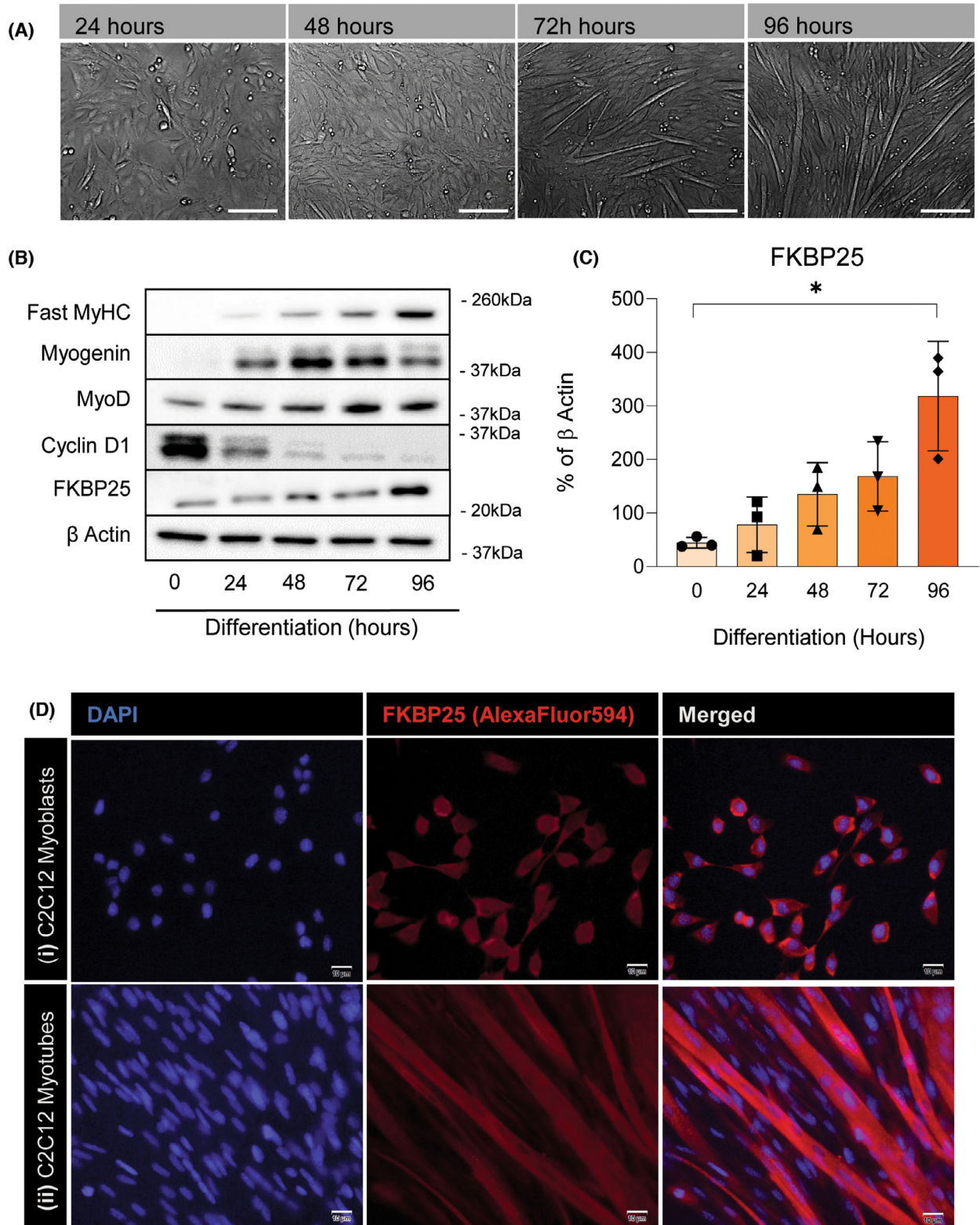


(Fig. 1B,C). Immunofluorescence analysis of myoblasts and differentiated myotubes showed that FKBP25 protein was predominantly localised to the cytoplasm, with a lower signal in the nucleus (Fig. 1D). These findings suggest that FKBP25 protein expression is related to differentiation status of the muscle cell, such that undifferentiated myoblasts expressed low levels of FKBP25, while differentiated myotubes express comparatively higher FKBP25 levels.

In contrast to post-mitotic myotubes, myogenic precursors cells can also exist as quiescent satellite cells. Satellite cells are the stem population within the skeletal muscle that enable regeneration in response to muscle damage [29]. Upon activation of satellite cells by injury, the cells divide to replenish their stem population, after which a daughter cell is able to migrate to the damaged site, fuse into the myofibres and initiate regeneration [30]. To examine whether FKBP25 expression is altered when quiescent myoblasts are activated to re-enter the cell cycle, a suspension culture was utilised to induce quiescence in myoblasts *in vitro*, followed by replating of these quiescent cells in high serum to induce proliferation. As shown in Fig. 2A, replating and differentiation of suspended myoblasts had no distinct impact of the time course of differentiation or morphology of the proliferating myoblasts or differentiated myotubes. Forty-eight hours of growth in suspension culture was associated with reduced Cyclin D1, consistent with a temporary withdrawal from the cell cycle and the induction of quiescence (Fig. 2B,C). Importantly, examination of FKBP25 protein revealed a marked decline in FKBP25 protein in the first 12 h after replating to a solid substratum in high serum conditions, which gradually recovered over 48 h of continued proliferation (Fig. 2C). These data suggest that FKBP25 expression may be required to be reduced to enhance the transition from quiescence to rapid proliferation on a solid surface. When combined with the differentiation data (Fig. 1), these results suggest that proliferation is associated with low levels of FKBP25 protein and that a reduction in FKBP25 may be required for efficient proliferation.

FKBP25 knockdown increases C2C12 myoblast accumulation/viability and migration *in vitro*

To further elucidate a potential role of FKBP25 in C2C12 myoblast proliferation and differentiation, an inducible FKBP25 knockdown (25KD) model was developed using SMARTvector doxycycline (Dox)-inducible lentiviral shRNA (Dharmacon, CO, USA). Following 72 h of treatment with $0.5 \mu\text{g}\cdot\text{mL}^{-1}$ of doxycycline, a 70% reduction of FKBP25 protein was

observed in C2C12 myoblasts containing mir2 treated with Dox (Fig. 3A,B). Considering our previous findings, we aimed to assess if levels of FKBP25 protein were, in fact, associated with enhanced proliferative capacity. To interrogate this hypothesis, 25KD C2C12 cells were subjected to a 5-day resazurin viability assay to assess cell accumulation over time. It was observed that, over time, there was a significant increase in cell viability of 25KD cells (Fig. 3C) and an increase in cell density, demonstrated by DiffQuick staining, at the 5d end point (Fig. 3D,E). Both these measures are consistent with an increase in cell proliferation; however, we cannot rule out that a 25KD-induced reduction in cell death also contributes to the increase cell accumulation. We next aimed to assess functional measures of 25KD myoblasts. Thus, using live cell imaging, a wound healing assay was performed to assess the impact of 25KD on cell migration *in vitro*. As shown in Fig. 3F,G, there was a significant increase in wound closure in 25KD myoblasts compared to control cells. These data suggest that a reduction in FKBP25 protein does indeed result in enhanced cell accumulation/viability and an increased migratory phenotype in C2C12 myoblasts.

FKBP25 knockdown does not alter microtubule post-translational modifications, impair tubulin stabilisation or the fraction of polymerised tubulin in C2C12 myoblasts

FKBP25 has recently been shown to be a microtubule (MT) binding protein that helps to promote MT stability by associating with the mitotic spindle during the telophase and cytokinesis stages of the cell cycle [23], with the knockdown of FKBP25 in U2OS cells resulting in a decrease in the fraction of stable microtubules, as assessed by a MT pelleting assay [23]. To investigate whether enhanced myoblast cell viability and migration may, in part, be due to decreased MT stability, subcellular fractionation was performed to assess the ratio of MTs to free tubulin. Under control and maximal polymerisation conditions (pre-treated with paclitaxel), the soluble fraction (S) represents less stable, dynamic MTs, while the pelleted fraction (P) represents the stable MTs [23]. Using this assay, we found that 25KD did not alter the relative proportion of MT polymerisation in C2C12 myoblasts under control (Fig. 4A) or forced polymerisation conditions (Fig. 4B). We also examined two tubulin post-translational modifications that can impact MT stability, alpha-tubulin acetylation and detyrosination, and found that these were not affected by 25KD (Fig. 4B,C–F). Finally, the expression of the MT depolymerising protein, stathmin, was also assessed and found not to be altered by 25KD (Fig. 4E,F). Combined, these data suggest that

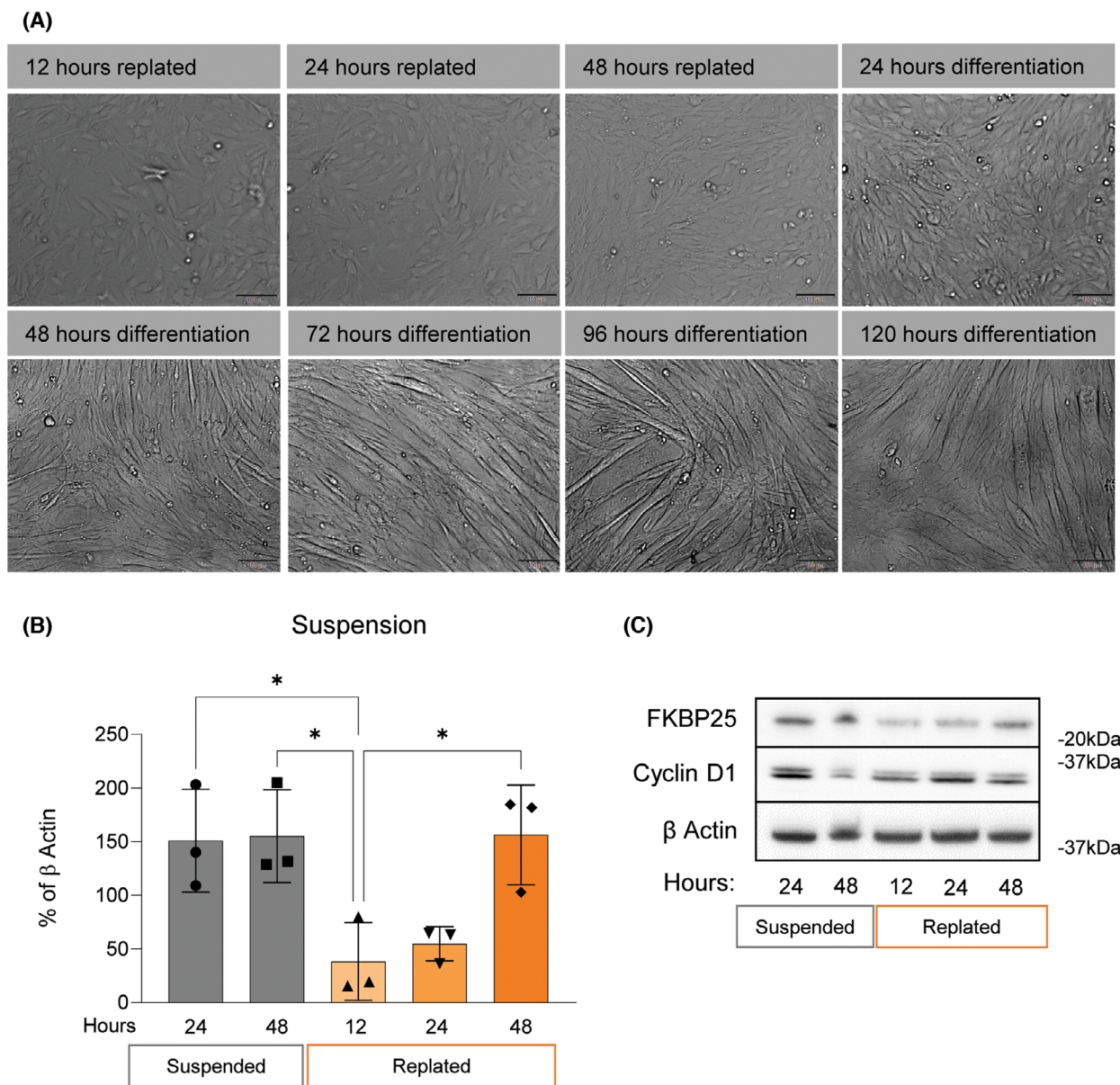


Fig. 2. FKBP25 protein is increased in quiescent myoblasts and reduced upon re-entry into the cell cycle. C2C12 myoblasts were suspended in a semi-solid medium (0.04%w/v methylcellulose/DMEM) for 48 h to enter a state of cell cycle arrest. (A) Upon removal from suspension culture, cells were replated on a standard tissue culture substratum. It was observed that there were no morphological changes to myoblasts or differentiated myotubes (Scale bar = 100 μ m). (B) FKBP25 protein expression is indifferent in suspended quiescent cells; however, it decreases once replated and allowed to re-enter the cell cycle. This is seen by an increase in Cyclin D expression. Represented by one-way ANOVA with Tukey's *post hoc* test. (C) Representative blots. Data are presented as mean \pm SD of $n = 3$, * = $P \leq 0.05$.

FKBP25 is not essential for regulation of MT dynamics in proliferating C2C12 myoblasts.

FKBP25 knockdown does not impair C2C12 myogenesis or myotube fusion

Next, we aimed to examine the impact of a reduction in FKBP25 on C2C12 myogenesis and myoblast fusion

during differentiation. Because Dox has previously been shown to inhibit C2C12 myoblast differentiation [31], we treated proliferating C2C12 myoblasts with Dox for 72 h to induce 25KD prior to differentiation. These 25KD cells were then differentiated for 120 h in the absence of Dox. Importantly, we found that the knockdown of FKBP25 in proliferating myoblasts was maintained throughout differentiation (Fig. 5A,E).

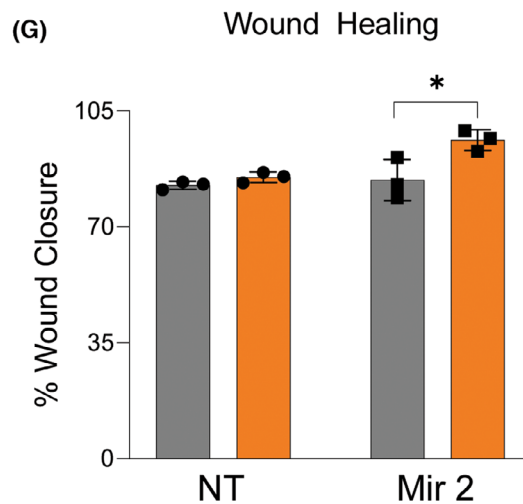
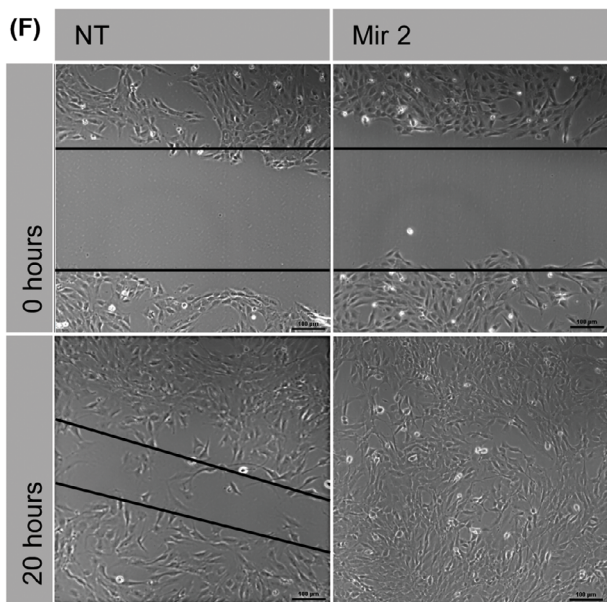
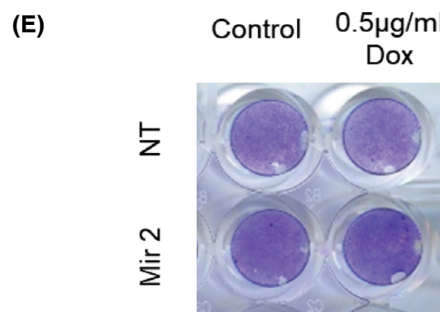
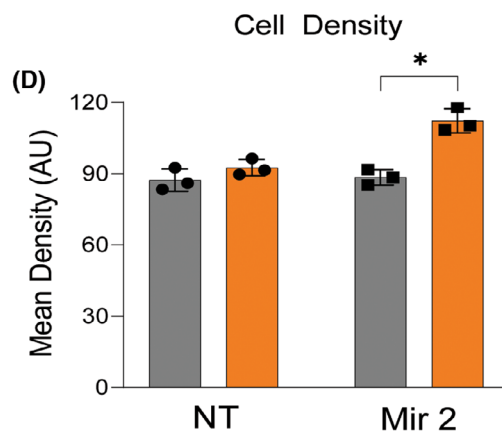
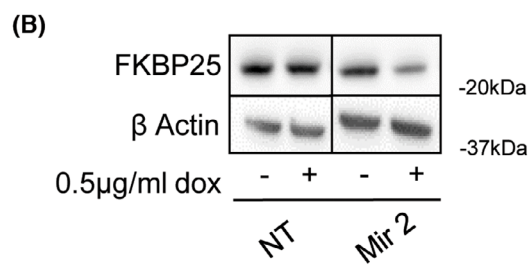
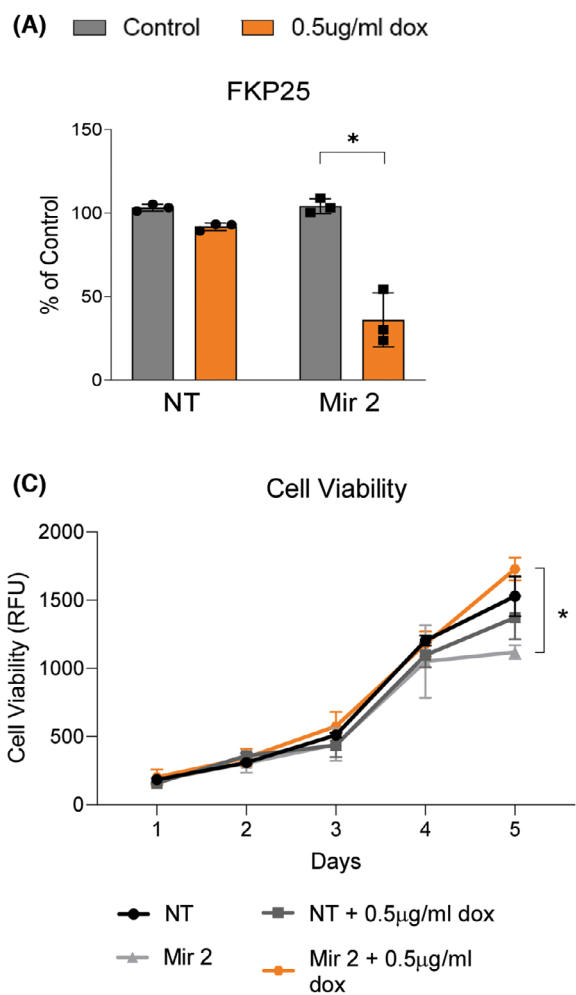


Fig. 3. FKBP25 knockdown increases C2C12 myoblast accumulation/viability and migration *in vitro*. Proliferating C2C12 myoblasts were transduced with lentiviral particles containing a plasmid expressing a doxycycline (Dox)-inducible shRNA (Mir2) that targets FKBP25 mRNA to knockdown FKBP25 protein expression or a non-targeting (NT) shRNA as the control. Transduced cells were selected and passaged every 2–3 days, for 10 days. Mir2 (and NT) expressing myoblasts were then treated with 0.5 $\mu\text{g}\cdot\text{mL}^{-1}$ Dox for 72 h, to induce FKBP25 knockdown (25KD). (A) Quantification and generation of 25KD using doxycycline-inducible shRNA in C2C12 myoblasts. (B) Representative Western blot showing reduced FKBP25 protein in Dox-treated and Mir2 expressing cells, compared to Dox-treated NT cells and untreated NT and Mir2 cells. (C) Dox-treated and untreated NT and Mir2 cells were seeded at low density and allowed to proliferate for 1–5 days, after which they were subjected to the AlamarBlue viability assay to assess the number of viable/proliferating cells. Upon 25KD there is a significant increase in cell viability over a 5-day period of active 25KD Mir 2. (D, E) After the AlamarBlue assays cells were stained with Diff-Quick stain and analysed for relative differences in cell density. Cell viability data is supported by density staining of cell accumulation over the same 5-day period. (F, G) Cells were plated at 90% confluence and left to adhere overnight before being scratched with a 200- μL pipette tip. The media was replaced with complete medium containing Mitomycin C to prevent proliferation during wound healing. Images were then captured every 15 min, and the percentage of wound closure (area in the wound μm^2) in 20 h was determined. Following 25KD C2C12 myoblast wound healing migration is enhanced such that Mir2 myoblasts close wound in 20 h compared to NT control, resulting in a 20% increase in wound healing (images taken at 10 \times magnification. Scale bar = 100 μm). Data presented as mean \pm SD of $n = 3$, * = $P \leq 0.05$.

Despite this, there were no observable differences in the expression of fast myosin heavy chain, myogenin, or MyoD, indicating no effect on differentiation (Fig. 5B–E). In support of this, 25KD had no effect on overall myotube morphology or myotube size (Fig. 6A,B). Moreover, fusion index (i.e. the number of nuclei/myotube) was found to be unaltered following 25KD (Fig. 6C/D). Combined, these data suggest that FKBP25 is unlikely to play an essential role in myoblast differentiation.

FKBP25 protein abundance is altered in *in vivo* models of skeletal muscle adaptation

Although we found no evidence that FKBP25 plays an important role in myoblast differentiation, it has recently been shown that FKBP25 protein is the most highly expressed FKBP in mature differentiated skeletal muscle *in vivo*, and this high expression places it just inside the top 10% of the most highly expressed proteins in the skeletal muscle proteome. This suggests that, although it may not be important for the process of differentiation, FKBP25 may still have an important role to play in the structure and/or function of differentiated muscle cells/fibres *in vivo*. Thus, to begin to explore this further, we examined whether FKBP25 abundance is altered in mature skeletal muscle undergoing adaptation to a range of different stressors. Firstly, we examined FKBP25 in two models of mechanically induced muscle hypertrophy. MTE and SA are forms of chronic mechanical loading, and we have shown that the MTE is a milder overload stimulus that induces less muscle damage/regeneration than the SA model [32,33]. As shown in Fig. 7A, FKBP25 was significantly increased 7 days after MTE and SA surgeries compared to sham muscles, suggesting that FKBP25 is upregulated during muscle growth. Next,

we examined FKBP25 expression in a mouse model of Duchenne muscular dystrophy (DMD), the mdx mouse. DMD is a severe type of muscular dystrophy induced by deletion of the dystrophin gene [34,35] which leads to increased susceptibility to mechanical stress resulting in repeated cycles of muscle damage and regeneration that lead to fibrosis, inflammation and pseudohypertrophy [36–38]. Similar to the MTE and SA models of muscle adaptation, FKBP25 was also upregulated in mdx muscle (Fig. 7B).

Finally, we examined FKBP25 in models of muscle atrophy. In the first model, denervation, where the muscle is unable to contract and undergoes a marked reduction in mechanical loading [39], we found that FKBP25 expression was reduced compared to sham controls (Fig. 7C). In the food deprivation model, muscle atrophy is due to reduced caloric intake which leads to reduced mTORC1 signalling and protein synthesis [39] and not to altered mechanical loading. In this model, we found that FKBP25 expression was not altered compared to ad lib fed controls (Fig. 7D). Combined, these studies demonstrate for the first time that FKBP25 expression dynamically regulated several models of skeletal muscle adaptation associated with muscle hypertrophy, atrophy and regeneration. This suggests that, in addition to a potential role in myoblast proliferation, FKBP25 may also play a role in the adaptation of mature skeletal muscle *in vivo*. These findings highlight the need for further *in vivo* loss- and gain-of-function studies to fully elucidate the role of FKBP25 in skeletal muscle *in vivo*.

Discussion

This is the first study to investigate the potential role of FKBP25 in skeletal muscle cells, showing that FKBP25 protein abundance is relatively low in

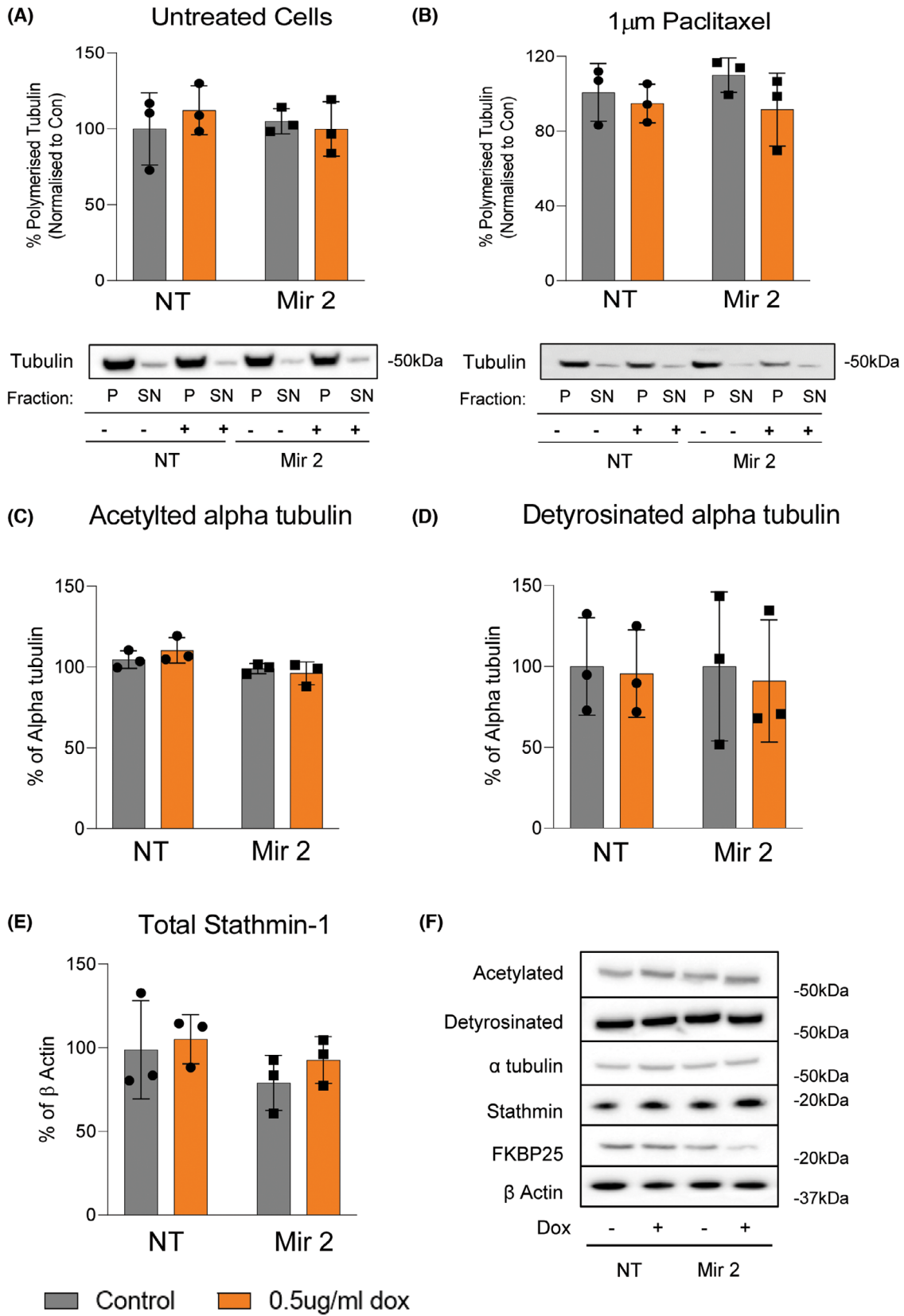


Fig. 4. FKBP25 knockdown in C2C12 myoblasts does not impair tubulin modifications associated with microtubule polymer stability, or the proportion of polymerised tubulin. Proliferating C2C12 myoblasts were transduced with lentiviral particles containing a plasmid expressing a doxycycline (Dox)-inducible shRNA (Mir2) that targets FKBP25 mRNA to knockdown FKBP25 protein expression or a non-targeting (NT) shRNA as the control. Transduced cells were selected and passaged every 2–3 days, for 10 days. Transduced cells were selected and passaged every 2–3 days, for 10 days. Mir2 (and NT) expressing myoblasts were then pre-treated with Dox for 72 h to induce FKBP25 knockdown (25KD) and plated at 80% confluency 24 h prior to the Microtubule/Tubulin *in vivo* assay (see Materials and methods section for details). (A) 25KD does not impair the proportion of polymerised tubulin in C2C12 myoblasts in either control or (B) paclitaxel-treated C2C12 myoblasts. (C/D) 25KD does not impair alpha-tubulin acetylation, or detyrosination in C2C12 myoblasts. (E) 25KD does not impact upon total microtubule catastrophe inducer, stathmin-1 in C2C12 myoblasts. (F) Representative Western blots. All data are presented as $n \pm SD$, $n = 3$.

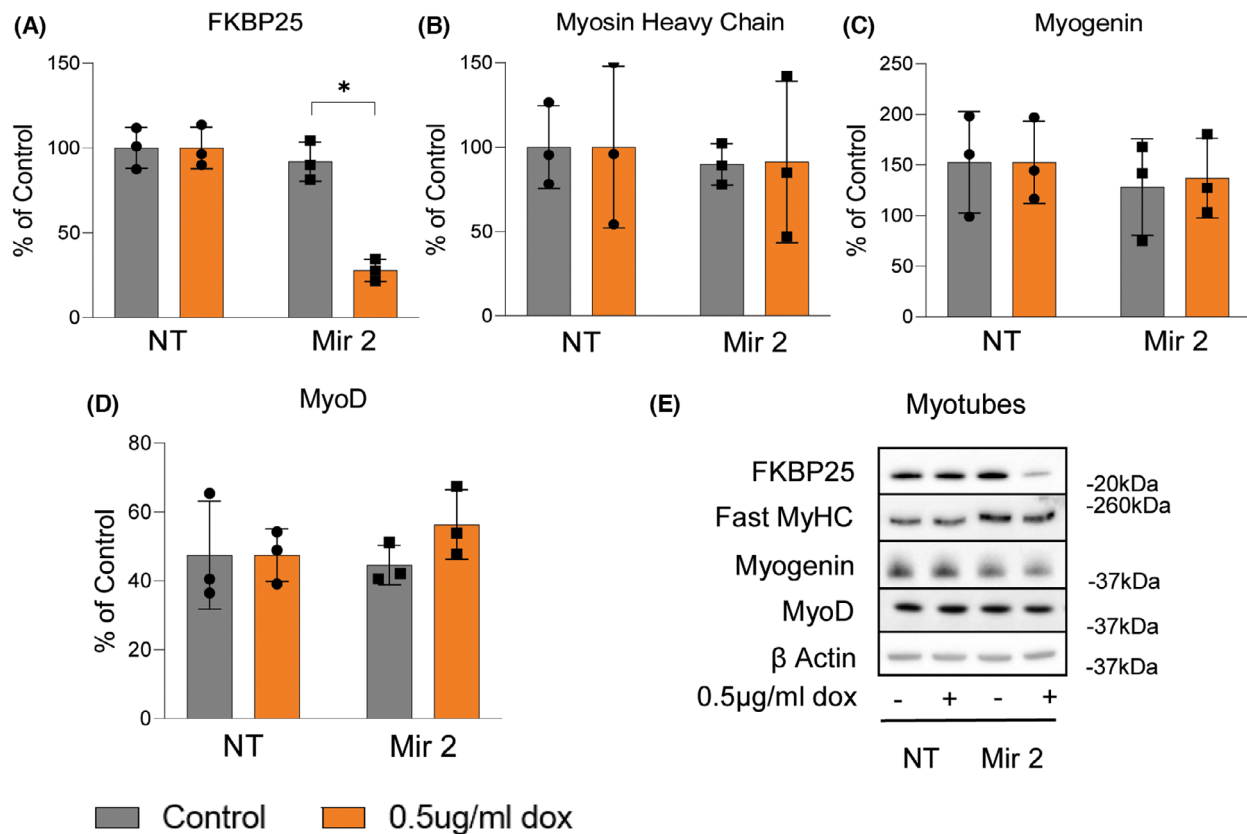


Fig. 5. FKBP25 knockdown does not impact upon features of myogenic differentiation or expression of myogenic regulatory factors. Proliferating C2C12 myoblasts were transduced with lentiviral particles containing a plasmid expressing a doxycycline (Dox)-inducible shRNA (Mir2) that targets FKBP25 mRNA to knockdown FKBP25 protein expression or a non-targeting (NT) shRNA as the control. Transduced cells were selected and passaged every 2–3 days, for 10 days. To induce FKBP25 knockdown in C2C12 myotubes, myoblasts were treated with 0.5 μ g mL⁻¹ doxycycline (Dox) in growth medium for 72 h prior to transition to differentiation medium containing 2% horse serum for up to 96 h. (A) 25KD knockdown in proliferating myoblasts was maintained throughout subsequent C2C12 differentiation. (B–E) 25KD did not impact the protein expression of differentiation markers, fast myosin heavy chain, myogenin or MyoD in differentiated C2C12 myotubes. All data are presented as mean \pm SD, $n = 3$, * = $P \leq 0.05$.

proliferating myoblasts, compared to differentiated myotubes and non-proliferating/quiescent myoblasts, suggesting that FKBP25 may need to be maintained at low levels to facilitate cell proliferation. This hypothesis is, in part, supported by our novel finding that a reduction in FKBP25 expression increased myoblast

accumulation/viability and migration. Interestingly, we found that a reduction in FKBP25 had no impact on *in vitro* myogenesis, despite FKBP25 abundance increasing during differentiation, suggesting that FKBP25 is not required for differentiation *per se*. Nonetheless, this differentiation-induced increase in FKBP25 is consistent

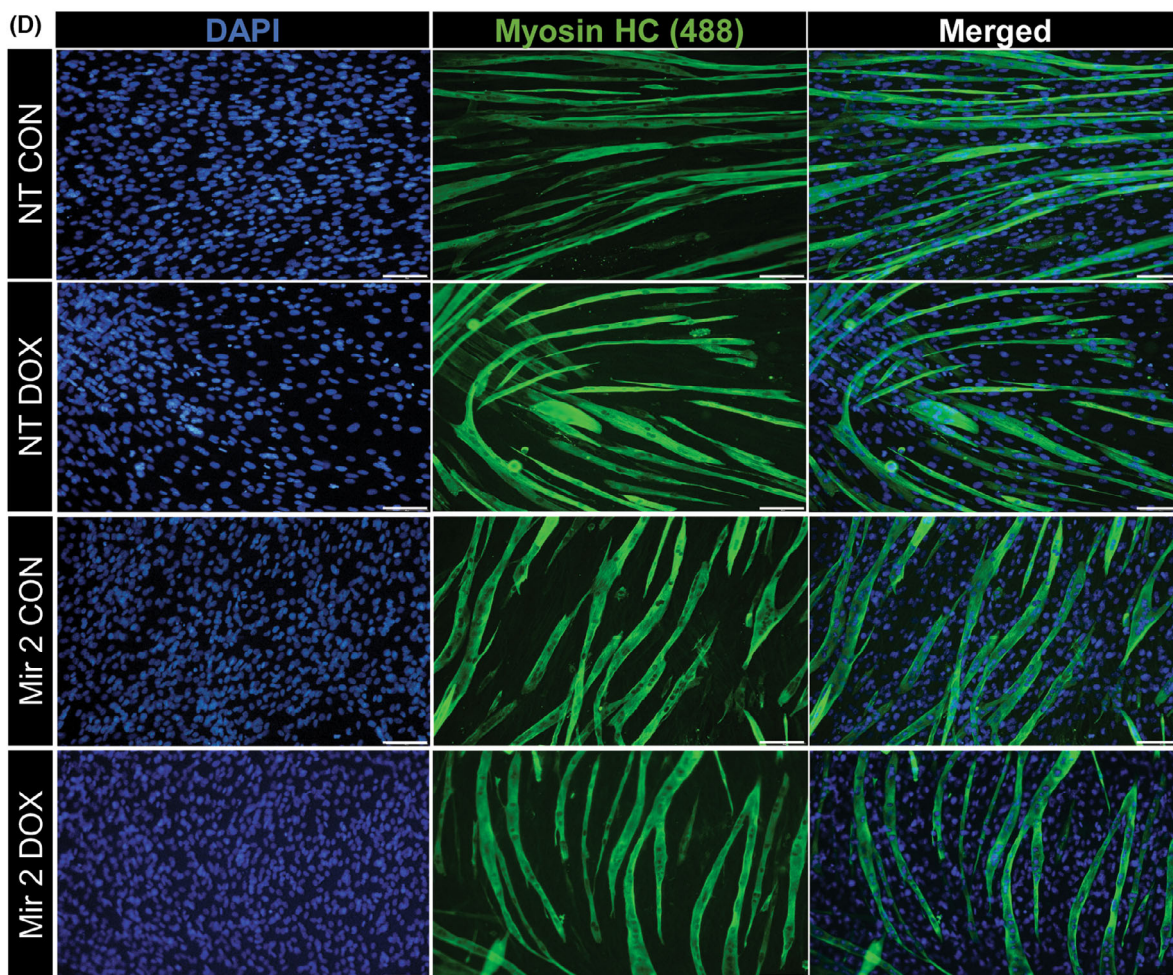
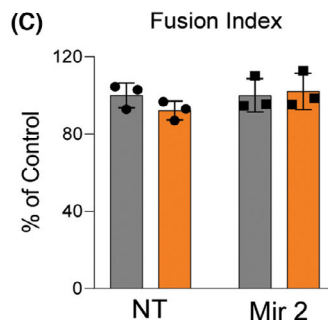
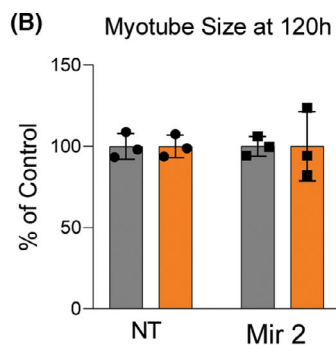
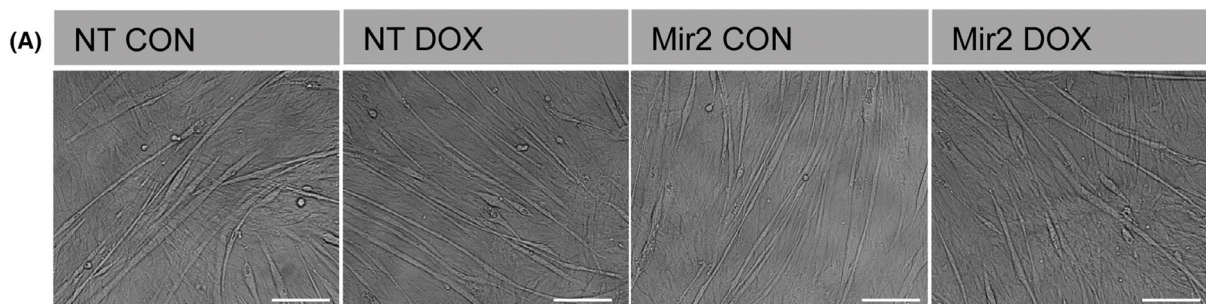


Fig. 6. FKBP25 knockdown does not impair myotube formation or fusion index of C2C12 myotubes *in vitro*. Proliferating C2C12 myoblasts were transduced with lentiviral particles containing a plasmid expressing a doxycycline (Dox)-inducible shRNA (Mir2) that targets FKBP25 mRNA to knockdown FKBP25 protein expression or a non-targeting (NT) shRNA as the control. Transduced cells were selected and passaged every 2–3 days, for 10 days. To induce FKBP25 knockdown in C2C12 myotubes, myoblasts were treated with 0.5 $\mu\text{g}\cdot\text{mL}^{-1}$ doxycycline (Dox) in growth medium for 72 h prior to transition to differentiation medium containing 2% horse serum for up to 96 h. (A) Myotube formation after 96 h of differentiation post 25KD resulted in no morphological alterations compared to NT control (images taken at 10 \times magnification. Scale bar = 100 μm). (B) Measurements of myotube size revealed no differences in myotube size upon 25KD. (C) Fusion index was calculated as number of nuclei per myosin HC-positive myofibre. (D) It was observed that 25KD did not impact upon fusion index (images taken at 60 \times magnification. Scale bar = 10 μm). All data are presented as mean \pm SD, $n = 3$.

with high levels of FKBP25 found in mature skeletal muscle *in vivo*, suggesting that FKBP25 may also play a role(s) in regulating skeletal muscle structure, function and/or adaptation. Indeed, we show for the first time that the abundance FKBP25 protein is dynamically regulated in a range of *in vivo* models of muscle adaptation. Overall, the findings of this study establish FKBP25 as a potential regulator of myoblast proliferation, with possible implications for satellite cell proliferation and migration and muscle regeneration, and as a potential regulator of skeletal muscle adaptation to *in vivo* stressors.

Our finding that FKBP25 protein increased during the differentiation of myoblasts initially suggested that this increase may be required for myogenesis; however, when FKBP25 was knocked down in myoblasts by ~70%, there was no impact on molecular or morphological markers of myoblast fusion or differentiation. Notwithstanding the possibility that the remaining ~30% of FKBP25 was sufficient to enable differentiation, these data suggest that FKBP25 is unlikely to play an important role in myogenesis. Given that under basal conditions, muscle stem cells *in vivo* (i.e. satellite cells) are typically found in a quiescent state and are activated to proliferate, migrate and fuse with existing muscle fibres in response to muscle damage [40], we assessed whether FKBP25 protein would be altered during the process of transitioning from a quiescent to a proliferative state. These experiments found that FKBP25 abundance rapidly decreased upon re-entry into the cell cycle and then gradually increased again as cell confluency increased. These data suggest that a reduction in FKBP25 may be required to facilitate the re-entry into the cell cycle and/or for accelerating proliferation. This hypothesis is supported by our finding that the knockdown of FKBP25 led to increased cell accumulation/viability. While our data suggest a time-dependent divergence for an observable change in 25KD cell accumulation, further studies would benefit from addition measurements to delineate the role of FKBP25 in promoting proliferation versus inhibiting apoptosis in the enhancement of cell accumulation.

This finding, however, contrasts with recent studies in transformed breast, lung and osteosarcoma cancer cell lines, in which FKBP25 expression is elevated, where the knockdown of FKBP25 reduced cell proliferation [23–25]. Together, these findings suggest that FKBP25's role in cell accumulation/viability may be cell type-specific and requires further investigation.

FKBP25 was recently identified as a microtubule (MT)-associated protein (MAP) that promotes MT polymerisation and stabilisation, with the knockdown of FKBP25 leading to disruption of the MT network in sarcoma-derived U2OS cells [23]. In the context of our finding that FKBP25 was reduced in myoblasts transitioning from a quiescent to a proliferative state, these findings could suggest that FKBP25 abundance may need to be reduced to allow for optimal MT dynamics required for high rates of proliferation, i.e. sustained elevated levels of FKBP25 may make MTs too stable and slow cell cycle progression. MTs also play roles in cell migration [41], and our finding that the knockdown of FKBP25 enhanced cell migration could similarly suggest that reduced FKBP25 optimises MT dynamics in a way that favours increased migration velocity. Although these hypotheses are attractive, we found no evidence of altered MT polymerisation, or changes to tubulin post-translational modifications that are associated with MT stability (acetylation or detyrosination) [42], with FKBP25 knockdown. This may, in part, be due to different levels of tubulin polymerisation in C2C12 myoblasts versus U2OS cells. Specifically, in the study of Dilworth *et al.* [23], the majority of tubulin was in the soluble non-polymerised fraction from U2OS cells, while we found most of the tubulin was in the insoluble polymerised fraction in C2C12 cells (Fig. 4A). Interestingly, the relative proportion of soluble to insoluble tubulin that we found in C2C12 myoblasts is similar to that reported for HELA, CG-4 cells and OE19 cell lines [43,44]. The reason for these cell type differences is not clear; however, they suggest the possibility of cell-specific differences in MT dynamics. Thus, while we cannot definitively rule out a role in the regulation of MT dynamics, other FKBP25-regulated

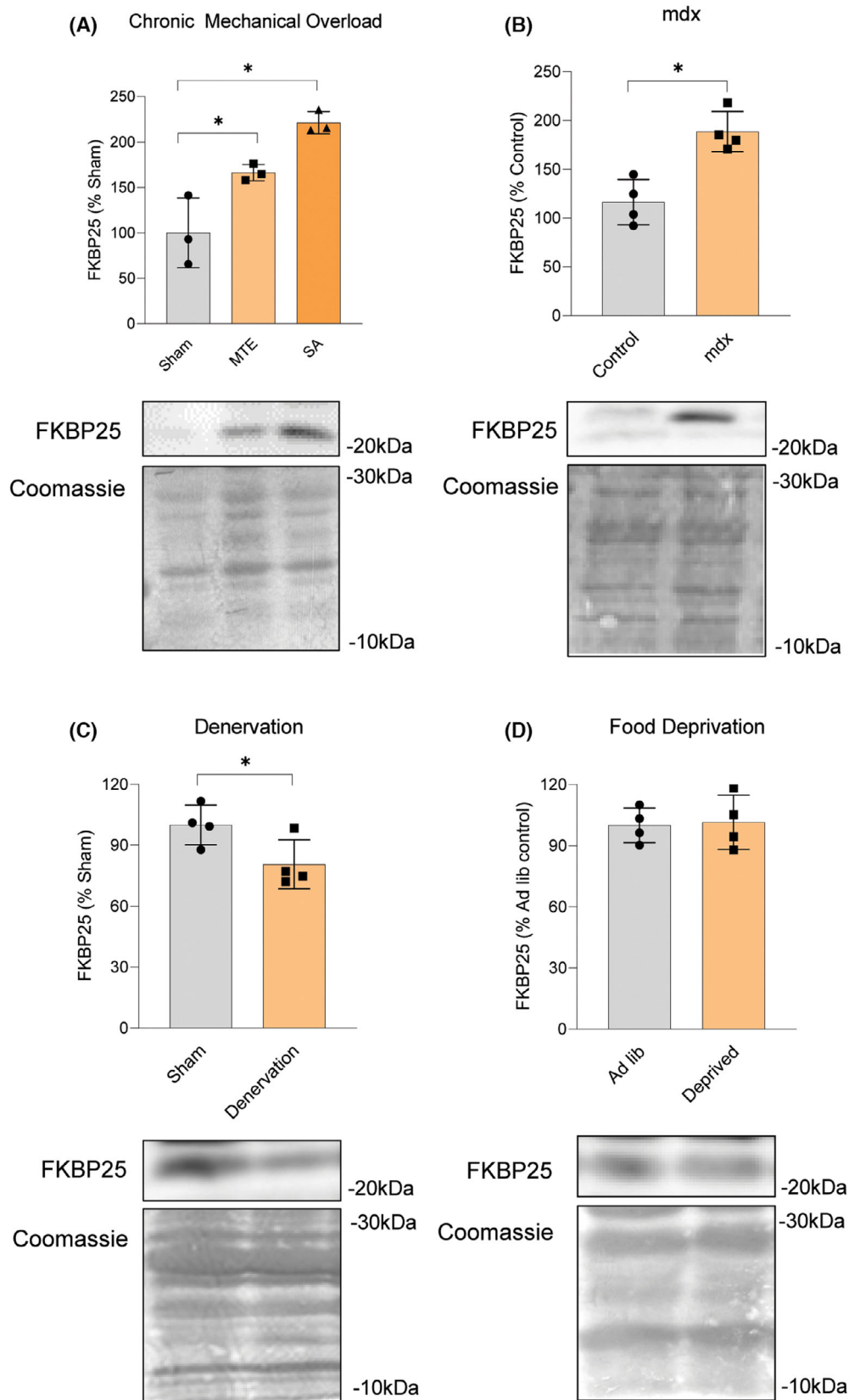


Fig. 7. FKBP25 protein expression is differentially expressed in *in vivo* models of skeletal muscle adaptations. (A) Female FVB/N mice were subjected to lower leg MTE or SA surgeries (or sham controls; see Materials and methods for details) to induce chronic mechanical overload and hypertrophy of the plantaris muscle over 7 days. FKBP25 protein expression is increased in both models of chronic mechanical loading (one-way ANOVA with Tukey's *post hoc* test). (B) Tibialis anterior (TA) muscles were dissected from male C57Bl/10ScSn (normal wild-type strain; Control) and C57Bl/10mdx (*mdx*) mice. FKBP25 protein expression is increased in *mdx* muscle tissue. (C) Female FVB/N mice were subjected to sciatic nerve denervation (or sham) surgery and the TA muscles were dissected 7 days post-surgery. FKBP25 protein expression is reduced in denervation-induced skeletal muscle atrophy. (D) Female FVB/N mice were subjected to 48-h food deprivation (or the control *ad libitum* diet; *ad lib*), after which TA muscles were dissected. FKBP25 protein is not altered in food deprivation-induced skeletal muscle atrophy. (B–D) Represented with unpaired *t*-tests. All data are presented as $n \pm SD$, $n = 3–4$, * = $P \leq 0.05$.

mechanisms are likely to play more substantial roles. One possibility is that FKBP25 is a MAP [23], but instead of regulating MT dynamics *per se*, it somehow regulates MT-mediated transport of cargo along the MTs, such as mRNA, rRNA and nascent proteins [45,46]. Therefore, a reduction in FKBP25 could lead to altered mRNA translation and/or protein localisation within the cell, leading to altered cell function. Clearly, further studies are required to elucidate a role for FKBP25, if any, in regulating MT-mediated intracellular transport.

Although we found no evidence that FKBP25 plays a key role in myogenesis *in vitro*, a recent quantitative proteomics analysis found that not only is FKBP25 the most highly expressed FKBP in mature differentiated mouse skeletal muscle *in vivo*, but its high expression levels places it in the top 10% most highly expressed proteins in the skeletal muscle proteome. This is an intriguing finding which suggests that, while FKBP25 may not be vital for the process of differentiation *per se*, it may still have an important role(s) to play in the structure and/or function of differentiated muscle fibres *in vivo*. Therefore, we began to investigate whether FKBP25 protein levels would be dynamically regulated in different *in vivo* models of muscle adaptation. These studies showed that FKBP25 protein was increased in two models of chronic mechanical loading [myotectomy (MTE) and synergist ablation (SA)] [33,39] and a model of chronic low-level muscle damage and regeneration [the *mdx* mouse model of Duchenne muscular dystrophy (DMD)] [47] but was decreased in the atrophic denervation model of reduced mechanical loading [39,48]. Whether these changes in FKBP25 are due to changes in transcription, mRNA translation and/or protein stability remains to be determined. Nonetheless, when combined, these data demonstrate that FKBP25 protein levels are dynamically regulated in muscles undergoing significant remodelling and changes in protein turnover. These findings prompt the question of what role (s) FKBP25 might be playing in models and adaptation? If FKBP25 does play a role in MT network

stability, it is interesting to note that muscles from adult dystrophic *mdx* mice have a denser microtubule structure than wild-type mice [49], which may necessitate higher levels of MAPs, including FKBP25. Denervation is also associated with significant reorganisation of the MT network [50,51]; however, the reduction of FKBP25 may be representative of reduced muscle fibre size and subsequent reduction in net density of the MT networks of atrophied muscle [52]. Conversely, the increase in FKBP25 with mechanical overload may simply be linked to the need for an increase in MTs with the expansion of muscle fibre size.

One feature that is common to the models in which FKBP25 levels were elevated (MTE- and SA-induced overload and *mdx* muscle) is an increase in protein synthesis and ribosome biogenesis [33,39,53]. In this context, and given its role as a peptide isomerase, it is perhaps not surprising that FKBP25 has been found to be associated with the pre-60S ribosomal subunit and with polyribosomes [21,54], the site of protein synthesis. Thus, an increase in FKBP25 may coincide with increased ribosomal biogenesis and may be required for an increase in protein synthesis. Arguing against this hypothesis, however, is the fact that FKBP25 was reduced in denervated muscle, despite the known associated increases in ribosomal biogenesis and protein synthesis [39,55]. FKBP25 was also recently shown to bind and inhibit the mTORC1 [56], a major regulator of protein synthesis and cell growth [57], whose signalling is known to be elevated in all four models in which FKBP25 was differentially regulated in this study (i.e. MTE, SA, *mdx* and Den) [33,39,48,53]. This could suggest that, at least in overloaded and dystrophic muscles, FKBP25 is part of a negative feedback loop to limit mTORC1 activation. In the case of denervation, however, the reduction in FKBP25 levels may be part of the mechanism that helps to increase mTORC1 activity and protein synthesis to attenuate the loss of muscle mass [39,48]. Further *in vivo* loss-of-function and gain-of-function studies are required to fully elucidate the function(s) of FKBP25 in mature skeletal muscle fibres.

In summary, this study shows that FKBP25 is a novel regulator of myoblast viability and migration, with potential implications for the regulation of satellite cell proliferation and migration in response to muscle damage. Furthermore, we found that FKBP25 protein abundance is differentially regulated in *in vivo* models of skeletal muscle hypertrophy, damage and regeneration, and atrophy, suggesting the potential for a role in muscle remodelling/protein turnover. Future mechanistic studies are now required to determine the role of FKBP25 in basal muscle structure and function, and in muscle adaptation.

Materials and methods

C2C12 myoblast culture

Mouse C2C12 myoblasts were cultured in Dulbecco's modified eagle medium (DMEM, Thermo Fisher, Waltham, MA, USA) supplemented with 10% foetal bovine serum (FBS), antibiotic/antimycotic (1%, Invitrogen, Carlsbad, CA, USA), Glutamax (1%, stable L-glutamine substitute, Thermo Fisher) and sodium pyruvate (1 mM per 110 mg·L⁻¹, Thermo Fisher), and HEPES (25 mM per 5.9 g·L⁻¹, Thermo Fisher). Cells were routinely tested for mycoplasma contamination using MycoAlert™ mycoplasma detection kit #LT07-318 (Lonza, Switzerland).

C2C12 differentiation

Cultures were maintained at low confluence to prevent premature differentiation. C2C12 myoblasts were differentiated by changing media to differentiation medium, DMEM containing 2% horse serum for up to 96 h.

C2C12 suspension culture to induce quiescence

C2C12 cells were grown to 70% confluency in T75 flasks and lifted as mentioned. A viscous suspension medium containing 4% methylcellulose/DMEM (V/W) prepared as previously described [58]. Cells were either collected from suspension or replated following 48 h in suspension.

Generation of shRNA knockdown of FKBP25 in C2C12 cells

C2C12 myoblasts were plated at 1×10^6 cells in a T25 flask (Corning, Mulgrave, Victoria, Australia) and allowed to adhere overnight at 37 °C with 5% CO₂. The growth medium was removed and replaced with 2 mL of DMEM containing lentiviral particles and 10 µg·mL⁻¹ of polybrene and incubated for 24 h. Following this, media was discarded and replaced with growth medium for a recovery period of 24 h. Cells were selected by puromycin antibiotic

resistance marker using 5 µg·mL⁻¹ puromycin (Sigma Aldrich, St. Louis, MO, USA) which was replaced or passaged every 2–3 days, for 10 days. To induce FKBP25 knockdown in C2C12 myotubes, myoblasts were treated with 0.5 µg·mL⁻¹ doxycycline (Dox) in growth medium for 72 h prior to transition to differentiation medium – as it is well established that the presence of Dox itself impairs myogenic differentiation [31]. shRNA sequences used for inducible FKBP25 knockdown include non-targeting (NT): TTTCAGTACCCTTAAAACG and Mir 3: AAACGAATCTGAACCGTGT. Mir2 for FKBP25 was selected from a set of miRNAs optimised and tested for FKBP25 knockdown in MD-MB-468 cells (not shown).

Tubulin polymerisation assay

The ratio of microtubule to free tubulin was determined using a Microtubule/Tubulin *In Vivo* Assay Biochem Kit (Cytoskeleton, CO, USA). In brief, cells were pre-treated with doxycycline to induce FKBP25 knockdown and played at 80% confluency 24 h prior to the assay. Each sample was treated with 1 µM of paclitaxel to induce polymerisation of the microtubules (MT) (1 h at 37 °C) as well as untreated control cells. All reagents were warmed to 37 °C unless otherwise specified. Cells were washed in PBS lysed and collected in 80 µL of buffer. Next, the supernatant from the low-speed spin was aliquoted into 1 mL of ultracentrifuge tubes and centrifuged at 100 000 g for 1 h at 37 °C. The supernatant from the ultracentrifugation contained the free tubulin fraction, and the pellet contained the polymerised MT fraction. The pelleted MTs were resuspended in 80 µL of MT stabilisation buffer, and 20 µL of 5× SDS buffer. 15 µL of 5× SDS buffer was added to the supernatant. The samples were left to stabilise at room temperature for 15 min before being subjected to SDS PAGE.

Immunofluorescence

Cells were grown on 150 µm thick poly-D-lysine coated glass coverslips (Nue Vitro Corporation, Vancouver, WA, USA), following treatment/induction of knockdown. Cells were fixed with 4% paraformaldehyde (PFA) at 37 °C for 5 min, followed by room temperature for 25 min. Fixed cells were washed five times with PBS. Cells were then incubated in blocking and permeabilising buffer (0.2% skim milk powder, 0.1 M glycine, 1% BSA, 0.01% triton-X in PBS) at room temperature for 30 min, followed by three PBS washes. The primary antibodies were made up in 0.1% BSA/PBST and incubated at room temperature for 60 min. The fluorophore-conjugated secondary antibodies were diluted in 0.1% BSA/PBS and incubated for 30 min at room temperature protected from light. Slides were washed five times in PBS and the nuclei counterstained with 1 µg·mL⁻¹ 4',6-diamidino-2-phenylindole (DAPI; Sigma Aldrich) for 10 min, and wash steps were repeated.

Slides were mounted with a coverslip using Fluoroshield anti-fade mounting media (Sigma Aldrich) and dried overnight before imaging with the BX53 Olympus microscope.

AlamarBlue viability assay

AlamarBlue (resazurin salt) viability assay (Sigma Aldrich) was used to measure viable, proliferating cells in a population. Seventy-two hours after initiating Dox-mediated FKBP25 knockdown, cells were resuspended at 1×10^4 cells·mL⁻¹ and seeded at 1000 cells per well and allowed to adhere overnight. AlamarBlue reagent was diluted 1 in 10 with growth medium and added to C2C12 plates followed by incubation protected from light at 37 °C with 5% CO₂ for 2 h. After the incubation period, the supernatant was transferred to a white opaque 96-well plate for fluorometric reading in the Varioskan Flash plate reader using SKANIT RE software (Thermo Fisher) at 580–610 nm (peak emission is 585 nm). The cells were replaced with fresh media and placed back into the incubator; this assay was repeated for 5 days. Measured relative fluorescence units (RFU) values were plotted for each time point.

Cell density measurements

At the end point of AlamarBlue assays, the cells were fixed and stained with Diff-Quick stain (Histolabs, Kew East, Victoria, Australia). The plates were then left to dry overnight and before being scanned for analysis. Mean relative density measurements were read using IMAGEJ (NIH; <http://rsb.info.nih.gov/nih-image/>) and normalised to non-dox-treated controls.

Wound healing assay

C2C12 cells were cultured and reseeded on a 6-well plate (Corning) at approximately 90% confluence. Cells were left to adhere overnight before being scratched with a 200- μ L pipette tip. The media was replaced with complete medium containing 5 ng·mL⁻¹ Mitomycin C (Sigma Aldrich) to prevent proliferation during wound healing. Coordinates were set within the scratch wound using NIS ELEMENTS software on the Nikon Eclipse Ti-E inverted widefield microscope (Nikon, Tokyo, Japan) to image each wound every 15 min for up to 24 h at 4 \times magnification. The images were compiled into a film clip and analysed using NIS ELEMENTS software (Nikon) to determine the wound closure time. Wound healing was analysed by determining the percentage of wound closure (area in the wound μ m²) in 20 h.

C2C12 protein extraction and Western blot analysis

Cells were plated in 6-well plates for protein extraction. Plates were placed on ice and rinsed with ice-cold PBS

before lysis with a modified radio-immunoprecipitation assay buffer (RIPA buffer – 1 mM EDTA, 0.5 mM EGTA, 10 mM Tris–HCl, 140 mM sodium chloride, 10% sodium deoxycholate and 1% Triton-X 100), containing protease and phosphatase inhibitor cocktails (Sigma Aldrich). Plates scraped using a cell scraper, and lysates were collected and triturated to shear any remaining cellular debris. Lysates were centrifuged, and the supernatants were collected. The protein concentration of lysates were quantified using bicinchoninic acid assay (BCA, Pierce Biotechnology, Rockford, IL, USA) using the Varioskan Flash plate reader using SKANIT RE software (Thermo Fisher) at 562 nm as per manufacturer's instructions.

Samples were prepared as per the manufacturer's instructions and electrophoretically separated on NUPAGE Novex 4–12% Bis-Tris precast gradient gels (Invitrogen). Gels were equilibrated in 20% ethanol and transferred onto a polyvinylidene difluoride (PVDF) membrane using the iBlot2 dry blotting system (Invitrogen). Membranes were blocked in 3% skim milk powder (w/v) in tris-buffered saline with 0.1% tween-20 (TBST, pH 7.4), washed and incubated in appropriate primary antibodies at 4 °C overnight. Following washing and secondary antibody incubation, membranes were imaged in the Vilber Lourmat imaging system (Vilber Lourmat, Eberhardzell, Germany). Densitometric measurements of the protein of interest were quantified using FUSION CAPT ADVANCE software (Vilber Lourmat). Upon analysis of protein expression results were normalised to a loading control (beta-actin) and expressed as either a proportion of beta-actin expression or normalised to non-dox-treated controls. The following primary antibodies were used: FKBP25 (WB; 1 : 3000, MAB3955, R&D Systems, Minneapolis, MN, USA), FKBP25 (IF; 1 : 500, ab16654, Abcam, Waltham, MA, USA), fast myosin heavy chain (1 : 3000, Ab51263, Abcam), myogenin (1 : 3000, Ab134175, Abcam), detyrosinated alpha-tubulin (1 : 1000, ab131368, Abcam), MyoD1 (1 : 1000, #13812, CST, Danvers, MA, USA), Cyclin D1 (1 : 3000, #55506, CST), beta-actin (1 : 5000, #4970, CST), Stathmin (1 : 1000, #13655, CST), acetylated alpha-tubulin (Lys40; 1 : 3000, #32–2700, Invitrogen), total alpha-tubulin (1 : 5000, sc-5286, Santa Cruz, Dallas, TX, USA) and pan tubulin (1 : 1000, #ATN02, Cytoskeleton, Denver, CO, USA). The following secondary antibodies were used: Anti-sheep HRP-conjugated (1 : 10 000, #GL21, Cytoskeleton), Goat anti-Rat IgG (H + L) HRP-conjugated (1 : 10 000, #PI-9400-1, Vector Labs, Newark, CA, USA), Goat anti-Mouse IgG (H + L) HRP-conjugated (1 : 10 000, A-10685, Invitrogen), Goat anti-Rabbit (H + L) IgG HRP-conjugated (1 : 5000, #32460, Invitrogen), Goat anti-Rabbit IgG (H + L) Cross-Adsorbed Alexa Fluor 594 conjugate (1 : 1000, A-11012, Invitrogen) and Goat anti-Mouse IgG (H + L) Cross-Adsorbed Alexa Fluor 488 conjugate (1 : 1000, A-11001, Invitrogen).

Animal models

All mice were purchased from Animal Resources Centre (ARC; Western Australia) and housed at the Western Centre for Health, Research and Education (WCHRE, Sunshine Hospital, Victoria, Australia) on a 12-h light/dark cycle with *ad libitum* access to food and water, unless otherwise stated. For mechanical overload (MTE and SA), denervation and food deprivation experiments, female FVB/N mice aged 8–11 weeks were used. For comparison between wild-type and dystrophic *mdx* mice, 3-week-old male C57Bl/10ScSn (normal wild-type strain; CON) and C57Bl/10mdx (*mdx*) were initially purchased and housed until 12 weeks of age before tissue collection. All experimental procedures were approved by the Victoria University Animal Ethics Committee and conformed to the Australian Code of Practice for the Care and Use of Animals for Scientific Purposes, 8th Edition, 2003.

Myotectomy and synergist ablation models of mechanical Overload-Induced muscle hypertrophy

To examine potential changes in FKBP25 protein abundance during *in vivo* models of adaptive muscle growth, mice were subjected to either sham, MTE or SA surgeries to induce chronic mechanical overload, as previously described [33,39]. Briefly, mice were anaesthetised with isoflurane, and immediately before the surgery mice were given an intraperitoneal (IP) injection of 0.05 mg·g⁻¹ of buprenorphine analgesic. To induce mechanical overload of the plantaris (PLT) muscles, bilateral MTE was performed under isoflurane anaesthesia by removing the distal tendon and myotendinous junction of the lower leg gastrocnemius muscle, as previously described [39]. For a more robust/stronger mechanical overload stimulus, SA surgeries were performed under isoflurane anaesthesia which the distal half of the gastrocnemius muscle and soleus muscle were removed as previously described [48]. Control mice were subjected to bilateral sham surgeries where an incision was made on the lower leg and then closed. Following the MTE and SA surgeries, incisions were closed with Vetbond surgical glue (Henry Schein, Melville, NY, USA). Mice were allowed to recover for 7 days, after which mice were re-anaesthetised with isoflurane and the PLT muscles were collected, immediately frozen in liquid N₂ and subjected to Western blot analysis as described below. Following tissue extraction, mice were killed by cervical dislocation while still under anaesthesia.

Denervation and food deprivation models of muscle atrophy

To examine potential changes to FKBP25 protein abundance in *in vivo* models of muscle atrophy *in vivo*, mice

were subjected to unilateral sciatic nerve denervation (Den) or 48-h food deprivation (FD). For denervation experiments, unilateral denervation surgeries were performed under isoflurane anaesthesia by making a small incision in the skin and underlying musculature on the lateral proximal thigh parallel with the femur, as previously described [39]. The sciatic nerve was then isolated, and a 3–4 mm section of the nerve was cut out. Control mice were subjected to a sham surgery. Following the surgeries, incisions were closed with Vetbond surgical glue. Mice were allowed to recover for 7 days, after which the tibialis anterior (TA) muscle was collected under isoflurane anaesthesia, frozen in liquid N₂ and subjected to Western blot analysis as described below. Following tissue extraction, mice were killed by cervical dislocation while still under anaesthesia.

For food deprivation experiments, food was withheld from mice for 48 h, with *ad libitum* access to water, as previously described [39]. Control mice were maintained on the *ad libitum* diet (AL). After 48 h, mice were anaesthetised with isoflurane and the TA muscles were collected, frozen in liquid N₂ and subjected to western blot analysis as described below.

mdx mouse model of Duchenne muscular dystrophy

For the collection of TA muscles from WT and *mdx* mice, mice first anaesthetised via IP injection of sodium pentobarbitone (60 mg·kg⁻¹) as previously described [47], after which muscles were frozen in liquid N₂ and subjected to Western blot analysis as described below. Following tissue extraction, mice were killed by cervical dislocation while still under anaesthesia.

Mouse muscle sample preparation and western blotting

Frozen muscles were homogenised with an Omni homogeniser (Model #TH220) for 20 s in ice-cold buffer A [40 mM Tris (pH 7.5), 1 mM EDTA, 5 mM EGTA, 0.5% Triton X-100, 25 mM β-glycerophosphate, 25 mM NaF, 1 mM Na₃VO₄, 10 mg·mL⁻¹ leupeptin and 1 mM PMSF]. The whole homogenate was used for further Western blot analysis. Sample protein concentration was determined with a DC protein assay kit (Bio-Rad, Hercules, CA, USA). Equivalent amounts of protein from each sample were dissolved in Laemmli buffer, heated to 100 °C for 5 min and then subjected to electrophoretic separation by SDS/PAGE. Following electrophoretic separation, proteins were transferred to a PVDF membrane and blocked with 5% powdered milk in TBS containing 0.1% Tween 20 (TBST) for 1 h followed by an overnight incubation at 4 °C with primary antibody dissolved in TBST containing 1% bovine serum albumin. After an overnight incubation, the

membranes were washed for 30 min in TBST and then probed with a peroxidase-conjugated secondary antibody (1 : 5000, #PI-1000, Vector Laboratories, Burlingame, CA, USA) for 1 h at room temperature. Following 30 min of washing in TBST, the blots were developed using ECL Prime reagent (Amersham, Piscataway, NJ, USA) and images were captured (Fusion FX imaging system, Vilber Lourmat). Densitometric analysis was performed using FUSION CAPT ADVANCE software (Vilber Lourmat). Membranes were then stained for total protein with Coomassie Blue. The signal for the band of the protein of interest was then normalised to the signal for total protein in each lane.

Statistical analysis

All C2C12 experiments were performed at least three times using biological replicates, and all biological replicates of functional data are representatives of three technical replicates. Animal experiments were represented as an $n = 4$, except MTE and SA which is represented by $n = 3$. Graph-Pad prism was used to analyse all data sets. All data sets were tested for normality using the Shapiro–Wilk test, and all data sets meet normality ($P > 0.05$). All experiments pertaining to doxycycline-inducible cell lines were analysed using a two-way analysis of variance (ANOVA). While treatments and conditions undertaken on parental cell lines were analysed with independent t -tests or one-way ANOVA depending on the variables, which is indicated throughout. Throughout the studies significance was reported at $P \leq 0.05$, and data were presented as mean \pm standard deviation.

Acknowledgements

None. Open access publishing facilitated by The University of Melbourne, as part of the Wiley - The University of Melbourne agreement via the Council of Australian University Librarians.

Conflict of interest

The authors declare no conflict of interest.

Author contributions

TC designed the project, performed all cell experiments and tissue analysis, performed statistical analysis and contributed to the manuscript; TRG contributed tissue from denervation and food deprivation animal studies; ER and CAT contributed tissue from mdx animal studies; JTP contributed to project design, conception of the project and manuscript editing; CAG contributed chronic mechanical loading animal tissues, project design and conception, and manuscript preparation. All

authors analysed and interpreted the data, revised it for critical intellectual content, and have approved the final version of the manuscript submitted for publication.

Data availability statement

The data that support the findings of this study are available from the corresponding author (craig.goodman@unimelb.edu.au) upon reasonable request.

References

- Fischer G & Schmid FX (1990) The mechanism of protein folding. Implications of in vitro refolding models for de novo protein folding and translocation in the cell. *Biochemistry* **29**, 2205–2212.
- Reimer U, Scherer G, Drewello M, Kruber S, Schutkowski M & Fischer G (1998) Side-chain effects on peptidyl-prolyl cis/trans isomerisation. *J Mol Biol* **279**, 449–460.
- Deber CM, Torchia DA, Wong SC & Blout ER (1972) Conformational interconversions of the cyclic hexapeptide cyclo(pro-Gly) 3. *Proc Natl Acad Sci USA* **69**, 1825–1829.
- Howe FS, Boubriak I, Sale MJ, Nair A, Clynes D, Grijzenhout A, Murray SC, Woloszczuk R & Mellor J (2014) Lysine acetylation controls local protein conformation by influencing proline isomerization. *Mol Cell* **55**, 733–744.
- Kubicek K, Cerna H, Holub P, Pasulka J, Hrossova D, Loehr F, Hofr C, Vanacova S & Stefl R (2012) Serine phosphorylation and proline isomerization in RNAP II CTD control recruitment of Nrd1. *Genes Dev* **26**, 1891–1896.
- Brichkina A, Nguyen NT, Baskar R, Wee S, Gunaratne J, Robinson RC & Bulavin DV (2016) Proline isomerisation as a novel regulatory mechanism for p38MAPK activation and functions. *Cell Death Differ* **23**, 1592–1601.
- Bonner JM & Boulianne GL (2017) Diverse structures, functions and uses of FK506 binding proteins. *Cell Signal* **38**, 97–105.
- Tong M & Jiang Y (2015) FK506-binding proteins and their diverse functions. *Curr Mol Pharmacol* **9**, 48–65.
- Mayer AD, Dmitrewski J, Squifflet J-P, Besse T, Grabensee B, Klein B, Eigler FW, Heemann U, Pichlmayr R, Behrend M *et al.* (1997) Multicenter randomized trial comparing tacrolimus (FK506) and cyclosporine in the prevention of renal allograft rejection: a report of the European tacrolimus multicenter renal study group. *Transplantation* **64**, 436–443.
- Brown EJ, Albers MW, Bum Shin T, Ichikawa K, Keith CT, Lane WS & Schreiber SL (1994) A mammalian protein targeted by G1-arresting rapamycin–receptor complex. *Nature* **369**, 756–758.

- 11 Li P, Ding Y, Wu B, Shu C, Shen B & Rao Z (2003) Structure of the N-terminal domain of human FKBP52. *Acta Crystallogr D* **59**, 16–22.
- 12 Zgajnar NR, De Leo SA, Lotufo CM, Erlejman AG, Piwien-Pilipuk G & Galigniana MD (2019) Biological actions of the Hsp90-binding immunophilins FKBP51 and FKBP52. *Biomolecules* **9**, 52.
- 13 Barent RL, Nair SC, Carr DC, Ruan Y, Rimerman RA, Fulton J, Zhang Y & Smith DF (1998) Analysis of FKBP51/FKBP52 chimeras and mutants for Hsp90 binding and association with progesterone receptor complexes. *Mol Endocrinol* **12**, 342–354.
- 14 Cindy R, Sinars JC-F, Rimerman RA, Scammell JG, Smith DF & Clardy J (2002) Structure of the large FK506-binding protein FKBP51 an HSP90 binding protein and a component of steroid receptor complex. *Proc Natl Acad Sci USA* **100**, 868–873.
- 15 Zhang X, Clark AF & Yorlino T (2008) FK506-binding protein 51 regulates nuclear transport of the glucocorticoid receptor β and glucocorticoid responsiveness. *Invest Ophthalmol Vis Sci* **49**, 1037–1047.
- 16 Peattie DA, Harding MW, Fleming MA, DeCenzo MT, Lippke JA, Livingston DJ & Benasutti M (1992) Expression and characterization of human FKBP52, an immunophilin that associates with the 90-kDa heat shock protein and is a component of steroid receptor complexes. *Proc Natl Acad Sci USA* **89**, 10974–10978.
- 17 Ward BK, Mark PJ, Ingram DM, Minchin RF & Ratajczak T (1999) Expression of the estrogen receptor-associated immunophilins, cyclophilin 40 and FKBP52, in breast cancer. *Breast Cancer Res Treat* **58**, 265–278.
- 18 Prakash A, Shin J, Rajan S & Yoon HS (2016) Structural basis of nucleic acid recognition by FK506-binding protein 25 (FKBP25), a nuclear immunophilin. *Nucleic Acids Res* **44**, 2909–2925.
- 19 Dilworth D, Upadhyay SK, Bonnafous P, Edoos AB, Bourbigot S, Pesek-Jardim F, Gudavicius G, Serpa JJ, Petrochenko EV, Borchers CH *et al.* (2017) The basic tilted helix bundle domain of the prolyl isomerase FKBP25 is a novel double-stranded RNA binding module. *Nucleic Acids Res* **45**, 11989–12004.
- 20 David Dilworth FG, Miller K & Nelson CJ (2019) FKBP25 participates in DNA double-strand break repair. *Biochem Cell Biol* **98**, 42–49.
- 21 Gudavicius G, Dilworth D, Serpa JJ, Sessler N, Petrochenko EV, Borchers CH & Nelson CJ (2014) The prolyl isomerase, FKBP25, interacts with RNA-engaged nucleolin and the pre-60S ribosomal subunit. *RNA* **20**, 1014–1022.
- 22 Jiang Q, Wu G, Yang L, Lu YP, Liu XX, Han F, Deng YP, Fu XC, Liu QB & Lu YM (2018) Elucidation of the FKBP25-60S ribosomal protein L7a stress response signaling during ischemic injury. *Cell Physiol Biochem* **47**, 2018–2030.
- 23 Dilworth D, Gudavicius G, Xu X, Boyce AKJ, O'Sullivan C, Serpa JJ, Bilenky M, Petrochenko EV, Borchers CH, Hirst M *et al.* (2018) The prolyl isomerase FKBP25 regulates microtubule polymerization impacting cell cycle progression and genomic stability. *Nucleic Acids Res* **46**, 2459–2478.
- 24 Liu P, Xie X, Yang A, Kong Y, Allen-Gipson D, Tian Z, Zhou L, Tang H & Xie X (2020) Melatonin regulates breast cancer progression by the lnc010561/miR-30/FKBP3 Axis. *Mol Ther Nucleic Acids* **19**, 765–774.
- 25 Zhu W, Li Z, Xiong L, Yu X, Chen X & Lin Q (2017) FKBP3 promotes proliferation of non-small cell lung cancer cells through regulating Sp1/HDAC2/p27. *Theranostics* **7**, 3078–3089.
- 26 Potts GK, McNally RM, Blanco R, You JS, Hebert AS, Westphall MS, Coon JJ & Hornberger TA (2017) A map of the phosphoproteomic alterations that occur after a bout of maximal-intensity contractions. *J Physiol* **595**, 5209–5226.
- 27 Li J, Wang Y, Wang Y, Yan Y, Tong H & Li S (2020) Fibronectin type III domain containing four promotes differentiation of C2C12 through the Wnt/ β -catenin signaling pathway. *FASEB J* **34**, 7759–7772.
- 28 Comai G & Tajbakhsh S (2014) Chapter one – molecular and cellular regulation of skeletal myogenesis. In *Current Topics in Developmental Biology* (Taneja R, ed.), pp. 1–73. Academic Press, Cambridge, MA.
- 29 Daneshvar N, Tatsumi R, Peeler J & Anderson JE (2020) Premature satellite cell activation before injury accelerates myogenesis and disrupts neuromuscular junction maturation in regenerating muscle. *Am J Physiol Cell Physiol* **319**, C116–C128.
- 30 Seale P, Poleskaya A & Rudnicki MA (2003) Adult stem cell specification by Wnt signaling in muscle regeneration. *Cell Cycle* **2**, 417–418.
- 31 Obradović H, Krstić J, Kukulj T, Trivanović D, Đorđević IO, Mojsilović S, Jauković A, Jovčić G, Bugarski D & Santibañez JF (2016) Doxycycline inhibits IL-17-stimulated MMP-9 expression by downregulating ERK1/2 activation: implications in myogenic differentiation. *Mediators Inflamm* **2016**, 2939658.
- 32 You J-S, McNally RM, Jacobs BL, Privett RE, Gundermann DM, Lin K-H, Steinert ND, Goodman CA & Hornberger TA (2019) The role of raptor in the mechanical load-induced regulation of mTOR signaling, protein synthesis, and skeletal muscle hypertrophy. *FASEB J* **33**, 4021–4034.
- 33 Goodman CA, Frey JW, Mabrey DM, Jacobs BL, Lincoln HC, You J-S & Hornberger TA (2011) The role of skeletal muscle mTOR in the regulation of mechanical load-induced growth. *J Physiol* **589**, 5485–5501.

- 34 Hoffman EP, Brown RH Jr & Kunkel LM (1987) Dystrophin: the protein product of the Duchenne muscular dystrophy locus. *Cell* **51**, 919–928.
- 35 Pons F, Augier N, Heilig R, Leger J, Mornet D & Leger JJ (1990) Isolated dystrophin molecules as seen by electron microscopy. *Proc Natl Acad Sci USA* **87**, 7851–7855.
- 36 Hughes KJ, Rodriguez A, Flatt KM, Ray S, Schuler A, Rodemoyer B, Veerappan V, Cuciarone K, Kullman A, Lim C *et al.* (2019) Physical exertion exacerbates decline in the musculature of an animal model of Duchenne muscular dystrophy. *Proc Natl Acad Sci USA* **116**, 3508–3517.
- 37 Gaglianone RB, Bloise FF, Ortiga-Carvalho TM, Quirico-Santos T, Costa ML & Mermelstein C (2020) Comparative study of calcium and calcium-related enzymes with differentiation markers in different ages and muscle types in mdx mice. *Histol Histopathol* **35**, 203–216.
- 38 Hori YS, Kuno A, Hosoda R, Tanno M, Miura T, Shimamoto K & Horio Y (2011) Resveratrol ameliorates muscular pathology in the dystrophic mdx mouse, a model for Duchenne muscular dystrophy. *J Pharmacol Exp Ther* **338**, 784–794.
- 39 Tabbaa M, Ruz Gomez T, Campelj DG, Gregorevic P, Hayes A & Goodman CA (2021) The regulation of polyamine pathway proteins in models of skeletal muscle hypertrophy and atrophy – a potential role for mTORC1. *Am J Physiol Cell Physiol* **320**, C987–C999.
- 40 Mauro A (1961) Satellite cell of skeletal muscle fibers. *J Biophys Biochem Cytol* **9**, 493–495.
- 41 Garcin C & Straube A (2019) Microtubules in cell migration. *Essays Biochem* **63**, 509–520.
- 42 Garnham CP & Roll-Mecak A (2012) The chemical complexity of cellular microtubules: tubulin post-translational modification enzymes and their roles in tuning microtubule functions. *Cytoskeleton* **69**, 442–463.
- 43 Tokési N, Lehotzky A, Horváth I, Szabó B, Oláh J, Lau P & Ovádi J (2010) TPPP/p25 promotes tubulin acetylation by inhibiting histone deacetylase 6. *J Biol Chem* **285**, 17896–17906.
- 44 Sauveteur J, Matera EL, Chettab K, Valet P, Guitton J, Savina A & Dumontet C (2018) Esophageal cancer cells resistant to T-DM1 display alterations in cell adhesion and the prostaglandin pathway. *Oncotarget* **9**, 21141–21155.
- 45 Denes LT, Kelley CP & Wang ET (2021) Microtubule-based transport is essential to distribute RNA and nascent protein in skeletal muscle. *Nat Commun* **12**, 6079.
- 46 Scarborough EA, Uchida K, Vogel M, Erlitzki N, Iyer M, Phyo SA, Bogush A, Kehat I & Prosser BL (2021) Microtubules orchestrate local translation to enable cardiac growth. *Nat Commun* **12**, 1547.
- 47 Timpani CA, Trewin AJ, Stojanovska V, Robinson A, Goodman CA, Nurgali K, Betik AC, Stepto N, Hayes A, McConell GK *et al.* (2017) Attempting to compensate for reduced neuronal nitric oxide synthase protein with nitrate supplementation cannot overcome metabolic dysfunction but rather has detrimental effects in dystrophin-deficient mdx muscle. *Neurotherapeutics* **14**, 429–446.
- 48 Goodman CA, Coenen AM, Frey JW, You J-S, Barker RG, Frankish BP, Murphy RM & Hornberger TA (2017) Insights into the role and regulation of TCTP in skeletal muscle. *Oncotarget* **8**, 18754–18772.
- 49 Khairallah RJ, Shi G, Sbrana F, Prosser BL, Borroto C, Mazaitis MJ, Hoffman EP, Mahurkar A, Sachs F, Sun Y *et al.* (2012) Microtubules underlie dysfunction in Duchenne muscular dystrophy. *Sci Signal* **5**, ra56.
- 50 Boudriau S, Cote CH, Vincent M, Houle P, Tremblay RR & Rogers PA (1996) Remodeling of the cytoskeletal lattice in denervated skeletal muscle. *Muscle Nerve* **19**, 1383–1390.
- 51 Ralston E, Lu Z & Ploug T (1999) The organization of the Golgi complex and microtubules in skeletal muscle is fiber type-dependent. *J Neurosci* **19**, 10694–10705.
- 52 Bruusgaard JC, Liestøl K & Gundersen K (2006) Distribution of myonuclei and microtubules in live muscle fibers of young, middle-aged, and old mice. *J Appl Physiol* **100**, 2024–2030.
- 53 Radley-Crabb HG, Marini JC, Sosa HA, Castillo LI, Grounds MD & Fiorotto ML (2014) Dystropathology increases energy expenditure and protein turnover in the mdx mouse model of Duchenne muscular dystrophy. *PLoS ONE* **9**, e89277.
- 54 Galat A & Thai R (2014) Rapamycin-binding FKBP25 associates with diverse proteins that form large intracellular entities. *Biochem Biophys Res Commun* **450**, 1255–1260.
- 55 Quy PN, Kuma A, Pierre P & Mizushima N (2013) Proteasome-dependent activation of mammalian target of rapamycin complex 1 (mTORC1) is essential for autophagy suppression and muscle remodeling following denervation. *J Biol Chem* **288**, 1125–1134.
- 56 Yang Y, Chen X, Yao W, Cui X, Li N, Lin Z, Zhao B & Miao J (2021) Esterase D stabilizes FKBP25 to suppress mTORC1. *Cell Mol Biol Lett* **26**, 50.
- 57 Goodman CA (2019) The role of mTORC1 in mechanically-induced increases in translation and skeletal muscle mass. *J Appl Physiol* **127**, 581–590.
- 58 Subramaniam S, Sreenivas P, Cheedipudi S, Reddy VR, Shashidhara LS, Chilukoti RK, Mylavarapu M & Dhawan J (2014) Distinct transcriptional networks in quiescent myoblasts: a role for Wnt signaling in reversible vs. irreversible arrest. *PLoS ONE* **8**, e65097.